



# Socioeconomic development role in hospitalization related to air pollution and meteorology: A study case in southern Brazil



Robson Will<sup>a</sup>, Marina Hirota<sup>b</sup>, Pedro Luiz Borges Chaffe<sup>c</sup>, Otavio Nunes dos Santos<sup>a</sup>, Leonardo Hoinaski<sup>c,\*</sup>

<sup>a</sup> Graduate Program in Environmental Engineering, Federal University of Santa Catarina, Florianópolis, Santa Catarina, Brazil

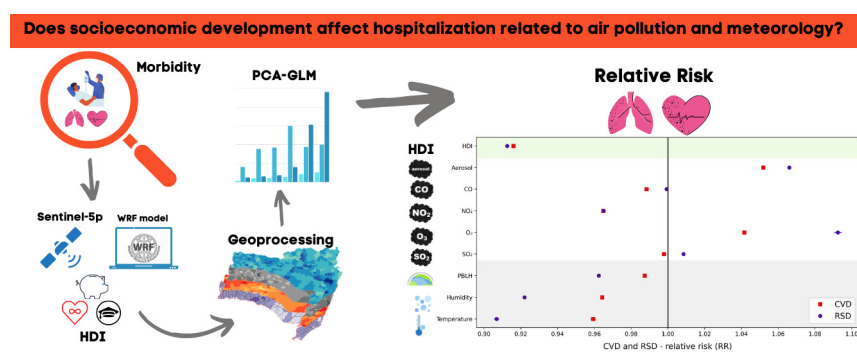
<sup>b</sup> Department of Physics, Federal University of Santa Catarina, Florianópolis, Santa Catarina, Brazil

<sup>c</sup> Department of Sanitary and Environmental Engineering, Federal University of Santa Catarina, Florianópolis, Santa Catarina, Brazil

## HIGHLIGHTS

- Sentinel-5p data is used in the analysis of air pollution related morbidity.
- Respiratory hospitalizations are more susceptible to meteorology and air pollution.
- Less developed municipalities are more prone to respiratory morbidity.

## GRAPHICAL ABSTRACT



## ARTICLE INFO

### Article history:

Received 20 October 2021

Received in revised form 17 February 2022

Accepted 17 February 2022

Available online 23 February 2022

Editor: Anastasia Paschalidou

### Keywords:

Air quality

Sentinel-5p

WRF

Human development index

Cardiorespiratory hospitalization

## ABSTRACT

Air pollution is one of the foremost environmental threats to human health. However, the meteorological and social factors that lead to respiratory and cardiovascular diseases have not been fully elucidated. In this study, we use Principal Component Analysis and Generalized Linear Model (PCA-GLM) to investigate the combined effect of socioeconomic development and air pollution on cardiorespiratory hospitalization in southern Brazil. This region has the highest rates of hospitalization by cardiorespiratory diseases in the country. We analyze three main sources of data: (i) air pollutants density from TROPOMI/Sentinel-5p satellite; (ii) temperature, humidity, and planetary boundary layer height (PBLH) modeled with the Weather Research Forecast model; and (iii) hospitalization by cardiorespiratory diseases obtained from the Brazilian National Health System. We estimate the Relative Risk (RR) using the PCA-GLM coefficients and inter-quartile variations of air pollutants density and meteorological parameters. Our results show that the population living in colder and drier municipalities is more prone to cardiorespiratory hospitalization. Regarding respiratory hospitalization, municipalities with lower socioeconomic development are more sensitive to meteorology and pollution variability than highly developed ones. In less developed municipalities, we observe the highest rates of cardiorespiratory hospitalization even if air pollution is low, which we interpret in terms of higher vulnerability. The RR analysis suggests that air pollution is an important environmental risk to cardiovascular diseases and respiratory diseases is more sensitive to air pollution and meteorology than cardiovascular ones. Our findings corroborate the mounting evidence that social vulnerability is a significant factor affecting the increase of cardiorespiratory hospitalization in the world.

## 1. Introduction

Air pollution is the world's major cause of cardiorespiratory diseases (WHO, 2017). Meteorological conditions can also impact human health and indirectly affect the cardiorespiratory morbidity by boosting air

\* Corresponding author.

E-mail address: [leonardo.hoinaski@ufsc.br](mailto:leonardo.hoinaski@ufsc.br) (L. Hoinaski).

pollution in events of atmospheric stagnation and lower planetary boundary layer height (PBLH) (Toro et al., 2019), with dry air and temperature extremes contributing to higher mortality by cardiovascular (CVD) and respiratory (RSD) diseases (Gasparrini et al., 2015). The effects of these environmental hazard are moderated by sex (Clougherty, 2010), lifestyle (Strak et al., 2017), age (Ebisu et al., 2019), and other social vulnerabilities (Pino-Cortés et al., 2020). The impacts of air pollution differ among socio-demographic groups (European Environment Agency, 2018), with vulnerable populations having a higher mortality risk usually as a result of greater exposure, higher sensitivity, and reduced ability to cope with the disease (European Environment Agency, 2018; Ho et al., 2018).

Although highly relevant to human health, the influence of air pollutant concentration (e.g., Gao et al., 2013; Krall et al., 2018) and meteorological conditions (e.g., Gasparrini et al., 2015; Ikäheimo et al., 2020) on cardiorespiratory hospitalization and mortality has generally been conducted using only local data. Even though monitoring stations are a reliable source of local data, their spatial representativity is usually limited (Righini et al., 2014) and does not capture the spatial variability of air pollutant concentrations at larger scales (Yatkin et al., 2020). The lack of spatially distributed air pollution data has been one of the limiting factors for detailed ecological epidemiology studies at regional scales (Requia et al., 2016).

Given that social, air pollution, and meteorological conditions are widely reported as critical drivers of cardiorespiratory diseases at the local scale (Laurent et al., 2007; Leitte et al., 2009), using datasets that expand the current fine-scale spatial coverage may enhance the understanding of the links among societal inequalities, environmental quality, and human health (European Environment Agency, 2018). In addition, the lack of methodological approaches to deal with data scarcity shared by most developing countries (Andréão and Toledo de Almeida Albuquerque, 2021) hinders the analysis of combined effects of multiple environmental health hazards (European Environment Agency, 2018). Recent high-resolution remote sensing products, like the Tropospheric Monitoring Instrument On-board Sentinel-5p, are a promising data source, which have not been fully employed for such studies.

Here, we perform a regional-scale analysis of the influence of air pollution, meteorology, and socioeconomic development on cardiorespiratory morbidity in Santa Catarina state (SC), Southern Brazil. We selected SC because it presents one of the highest hospitalization rates for cardiorespiratory diseases in Brazil (Brasil, 2020). The dataset comprises a combination of satellite images of air pollutant density, meteorological variables from regional model outputs, and hospitalization data for municipalities.

## 2. Methodology

### 2.1. Study area

We evaluate the effect of air pollution and meteorological conditions on cardiorespiratory hospitalization using the state of SC in Southern Brazil as a study case. The state is 95,300 km<sup>2</sup> (Fig. 1) with a humid subtropical climate, according to the Köppen-Geiger classification (Alvares et al., 2013). Average annual temperatures range from 18 to 22 °C at lower altitudes (0-400 m) and from 12 to 18 °C at higher altitudes (>400 m) (Fig. 1a).

In this work, socioeconomic development for each municipality of SC is characterized using the 2010 Human Development Index (HDI) obtained from the Brazilian Institute of Geography and Statistics (IBGE, 2013). The United Nations Program for Development – Brazil (UNPD-Brazil) in collaboration with the Institute of Applied Economic Research and João Pinheiro Foundation developed the HDI municipal dataset, using an adaptation of the global HDI method with the same dimensions considering local variables and available data. The HDI index takes into account three dimensions: (i) life expectancy at birth to measure a long and healthy life; (ii) average per capita family income to estimate the standard of living; and (iii) mean years of schooling for adults aged 25 years and older and the expected years of schooling for children of school-going age as a measurement of access to education (IBGE, 2013).

The coastal areas of SC are characterized by moderate to high HDI and a tourism economy (Fig. 1b). The Northern and Southern regions are the mostly industrialized, consequently, with higher SO<sub>2</sub> density (Fig. 1c). In the central part of SC is observed the lowest HDI, especially far from major cities (de Rocha, 2019). In this analysis, we have considered 293 out of 295 municipalities in Santa Catarina state. Two municipalities have been excluded from the analysis because they are not listed in the available shapefile used to delineate the municipalities' boundaries. Table 1 presents basic descriptive information of Santa Catarina's municipalities.

### 2.2. Air quality data

Air pollutant densities of CO, NO<sub>2</sub>, SO<sub>2</sub>, Aerosol, and O<sub>3</sub> in the tropospheric vertical column are obtained from the Tropospheric Monitoring Instrument (TROPOMI) onboard the Copernicus Sentinel 5 Precursor (S5P) satellite (<https://www.copernicus.eu/en>). We sample daily data with 7 km (along) × 3.5 km (across) resolution for the year 2019 using the Earth Engine data catalog (<https://developers.google.com/earth-engine/datasets/catalog/sentinel-5p>). We consider monthly 90<sup>th</sup> percentile

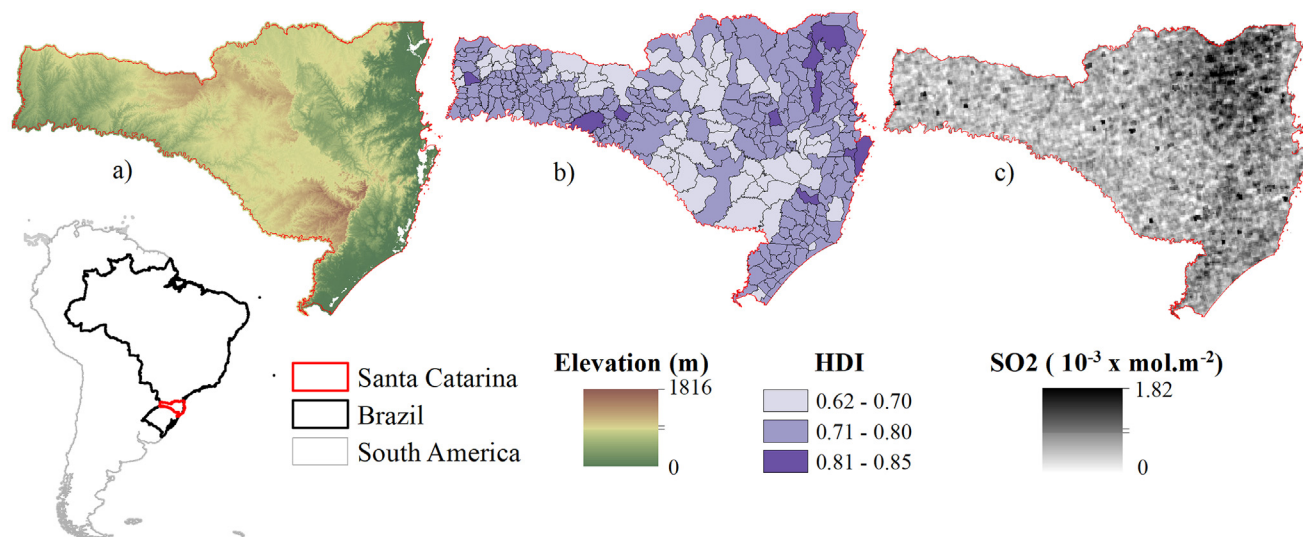


Fig. 1. Geographical location of Santa Catarina State. (a) terrain elevation, (b) Human development index (HDI) for each city. (c) median density of SO<sub>2</sub> in 2019 using Sentinel-5p data. Santa Catarina highlighted in red in Brazil

**Table 1**  
Descriptive information of the data used in this work from 293 of 295 Santa Catarina's municipalities.

	25th quantile	50th quantile	75th quantile
Population form municipalities	3642	7877	18,950
HDI	0.71	0.74	0.76
Morbidity RSD for 100 k inhabitants	42.74	72.53	133.39
Morbidity CVD for 100 k inhabitants	42.17	63.33	95.26
Temperature (°C)	16.44	20.06	22.12
Humidity (kg/kg)	9.49	12.17	13.36
PBLH (m)	352.87	438.57	510.07
Monoxide carbon (mol/m <sup>2</sup> ) x 10 <sup>-2</sup>	2.38	2.63	2.95
Ozone (mol/m <sup>2</sup> ) x 10 <sup>-1</sup> (25–50-75)	1.16	1.2	1.26
Nitrogen dioxide (mol/m <sup>2</sup> ) x 10 <sup>-5</sup>	5.66	6.32	6.78
Sulfur dioxide (mol/m <sup>2</sup> ) x 10 <sup>-4</sup>	2.78	4.17	6.05
Aerosol (UV Aerosol index)	0.8	0.95	1.09

of air pollutant density to affect human health and aggregate it by the municipality, matching the spatial and temporal scales of hospitalization data. Fig. 2 shows the municipal mean annual values of monthly 90° percentile from TROPOMI data in SC. Higher densities of NO<sub>2</sub> and O<sub>3</sub> are found in the South of SC, while that of SO<sub>2</sub> and CO are found in the North. Winter and spring are the seasons in which the air pollutant density is higher in Santa Catarina (Fig. 2 a-e).

The European Space Agency (ESA) provides a validation of the Sentinel-5 mission at <https://mpc-vdaf.tropomi.eu/>, containing a comparison with independent satellite missions and ground-level monitoring. The last report from this platform compares TROPOMI and ground level measurements using data from 25 monitoring sites from July to September 2021, revealing a bias of + 16% for O<sub>3</sub> and – 34% for NO<sub>2</sub>. CO density from TROPOMI has a bias around + 6.5%. Goldberg et al. (2019) show that TROPOMI overestimates 22% the concentration of CO when compared with data from 3 monitoring sites in New York, while an underestimation of 21% was observed in Toronto. Although independent comparisons have demonstrated bias in air pollutant densities from TROPOMI, these measurements are well correlated with observations (e.g., Zhao et al., 2021; Borsdorff et al., 2018).

### 2.3. Meteorological data

We run the Weather Research Forecast (WRF) model version 4.0 (Skamarock et al., 2019) to get gridded meteorological data within SC for 2019. We extract temperature, air humidity and planetary boundary layer height (PBLH) using the WRF outputs. We used WRF outputs since other gridded meteorological databases do not provide high resolution and PBLH data. The simulations are performed with two nested modeling domains with 15 × 15 km (d01) and 3 × 3 km (d02) (Appendix 01). One-way nesting provides a higher model performance, where the initial and lateral boundary conditions for the finer grid are obtained from the coarse grid. To improve the estimates of PBLH, we adopt the maximum number of vertical levels (33 levels of 50 hPa) in the WRF simulations. Other WRF physics parameterizations we adopt: Morrison 2-moment scheme for microphysics; Rapid radiative transfer model (RRTM) for a longwave spectral region; Dudhia scheme for shortwave radiation; Monin-Obukhov Similarity scheme for surface-layer; Noah Land-Surface Model for land-surface; YSU scheme for boundary layer, and Kain-Fritsch scheme for cumulus.

Global meteorological data from the Global Forecast System (GFS) provided by the National Center for Environmental Prediction (NCEP) with a spatial resolution of 0.5° x 0.5° and temporal resolution of 6 h (<https://www.ncdc.noaa.gov/data-access/model-data/model-datasets/global-forecast-system-gfs>) is set as boundary and initial conditions in WRF simulations (Skamarock et al., 2008). Land use for WRF is obtained from Moderate Resolution Imaging Spectroradiometer (MODIS) with the classification scheme United States Geological Survey (USGS) ([https://www2.mmm.ucar.edu/wrf/src/wps\\_files/geog\\_high\\_res\\_mandatory.tar.gz](https://www2.mmm.ucar.edu/wrf/src/wps_files/geog_high_res_mandatory.tar.gz)).

We calculate monthly averaged values for each municipality in SC from WRF hourly outputs to coincide with the temporal resolution of hospitalization data. Fig. 2 shows temperature, humidity, and PBLH within SC's municipalities for 2019. There is a clear seasonality in temperature, air humidity, and PBLH (Fig. 2 f-h). An interannual variation of 10 °C is observed in median temperature values. Temperature and specific humidity spatial patterns in SC are similar and driven mainly by topography. The center and western region of SC present the lowest values of PBLH, implying in lower dispersion of air pollutants.

### 2.4. Hospitalization and HDI data

Hospitalization by cardiorespiratory diseases data is obtained from the Department of Informatics from the Brazilian National Health System (DATASUS) (<http://www2.datasus.gov.br/DATASUS/index.php?area=02>). We select the morbidity cases for cardiovascular diseases (CVD, codes ICD-10 and I00-I99) and respiratory diseases (RSD, codes ICD-10 and J00-J99) occurring in 2019. We use RSD and CVD monthly data aggregated by municipality. Municipality population data from the Brazilian National Institute of Statistics and Geography (IBGE, 2020) is used to calculate the hospitalization rate per 100.000 inhabitants. A moderate seasonality is observed in cardiorespiratory hospitalizations in SC (Fig. 2 i-g), with higher values of the cardiorespiratory disease occurring in winter. Hospitalization data are normalized by population in this manuscript.

We adopt the same municipal HDI classification (very low, low, medium, high, and very high) as recommended by the UNPD-Brazil (PNUD, Ipea, 2013). The municipalities are grouped using HDI ranges of middle (0.6 to 0.7), high (0.7 to 0.8), and very high (>0.8) levels of development and the Mann-Whitneys post hoc test evaluates the variability of each group.

### 2.5. Statistical analysis

We use Spearman ranking to analyze the correlation among air pollutants density, meteorological conditions, hospitalizations, and HDI. Because correlation analysis can mask the effects of confounding variables, we also apply the combination of Principal Component Analysis and Generalized Linear Model (PCA-GLM; as presented by Sun et al., 2019) to evaluate the effect of meteorological parameters and air pollutants concentration on the RSD and CVD hospitalizations. The PCA-GLM resolves the collinearity interference between the variables (in our case air pollutants density, meteorological conditions, hospitalizations). We employ the air pollutant density from Sentinel-5 and meteorological output from WRF as original variables in the PCA-GLM, grouping municipalities in the same HDI range.

Before employing the PCA-GLM, we standardize and normalize the covariates (air pollution density, meteorology data, and HDI) (Appendix 2). Since we use Poisson regression, the response variable does not require standardization and normalization. We visually inspected the residual autocorrelation from the PCA-GLM through Autocorrelation Function (ACF) and Partial Autocorrelation Function (PACF) plots of Pearson residuals (Appendix 3 A). Identified serial correlations in the residual have been removed by fitting Autoregressive Integrated Moving Average (ARIMA) model to residual and added as a further covariate in Poisson regression (Appendix 3 BC). This procedure has been used to account for the confounding covariates (Tobías and Saez, 2004). The Pearson residual graphs after including the ARIMA confirm that the removal serial correlation from the analysis (Appendix 3 D).

PCA transforms the original variables into a new and smaller set of variables, called principal components (PCs). The PCs are orthogonal linear combinations of the original variables which explain the original variance and covariance. Since the PCs are orthogonal to each other, they can be used in multivariate models including all variables in the same model without misinterpretation of regression coefficients due to the collinearity

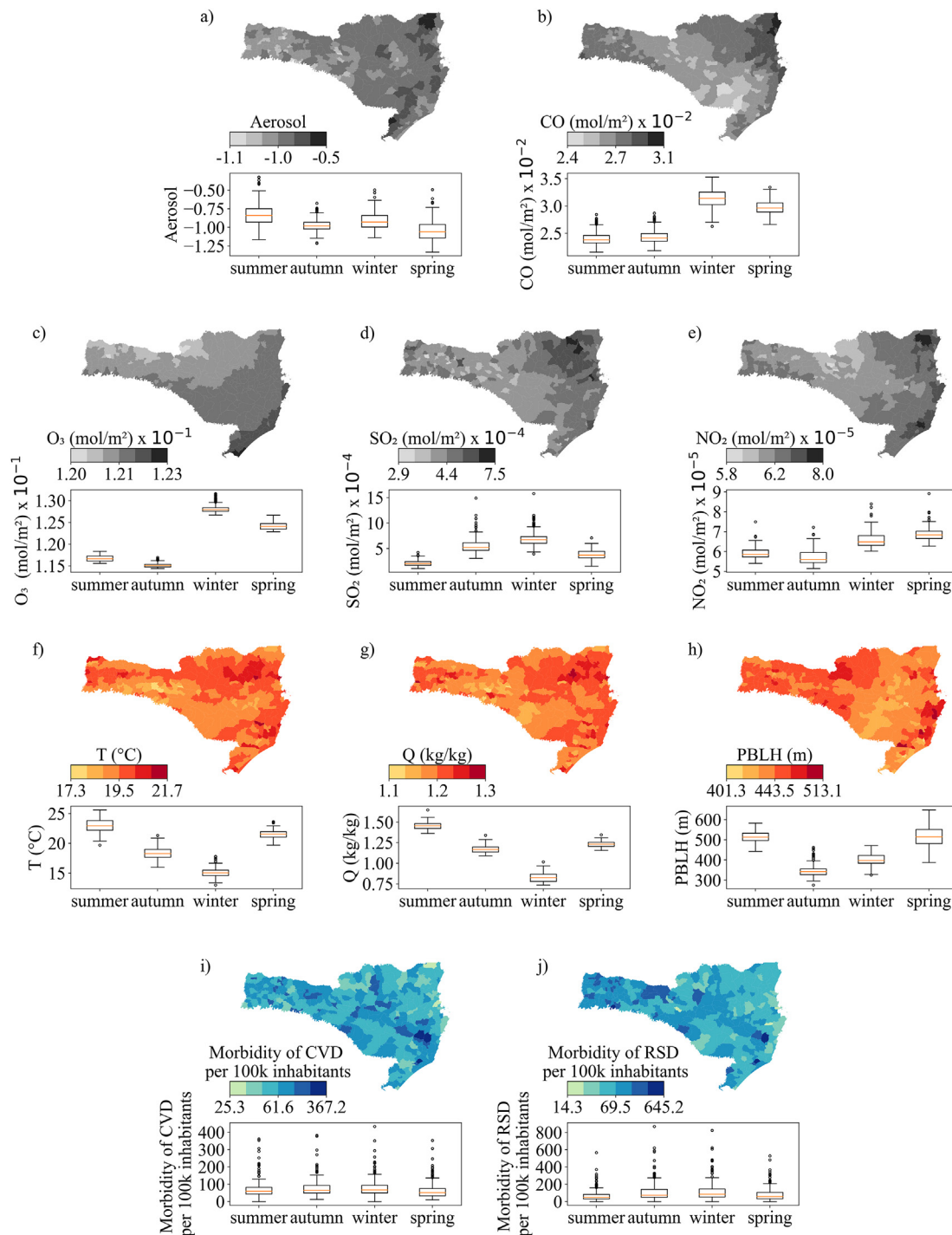


Fig. 2. Spatial distribution in 2019 of a) aerosol, b) CO, c) O<sub>3</sub>, d) SO<sub>2</sub>, e) NO<sub>2</sub>, f) T (temperature), g) Q (specific humidity), h) PBLH, i) CVD, and j) RSD. Data from Sentinel-5 (a-e), WRF outputs (f-h), and DATASUS (i-j). We used annual average from 90<sup>th</sup> percentile monthly values in a-e) and annual averages f-h). Boxplot shows the seasonal variability of each variable from a-j).

effect. Spearman correlation analysis confirms the orthogonality among PCs (*p*-values larger than 0.05 Appendix 04). Given a mean-centered dataset *X* with *n* samples and *p* original variables (CO, O<sub>3</sub>, SO<sub>2</sub>, NO<sub>2</sub>, aerosol, T, Q, PBLH), the component that retains the maximum variance of data is the first principal component (PC1) is given by the linear combination of the original variables CO, O<sub>3</sub>, SO<sub>2</sub>, NO<sub>2</sub>, aerosol, T, Q, PBLH, according to:

$$PC1 = \alpha_1 CO + \alpha_2 O_3 + \alpha_3 SO_2 + \alpha_4 NO_2 + \alpha_5 aerosol + \alpha_6 T + \alpha_7 Q + \alpha_8 PBLH \quad (1)$$

The covariance matrix (*S*) given by:

$$S = \frac{1}{n - 1} X'X \quad (2)$$

where *X* is an (*n* × *p*) matrix.

It is not possible to formally include HDI into the PCA-GLM model since meteorological and air pollution density are monthly data while HDI data a single decadal value. Using the hospitalization data as the response variable and the PCs in a Poisson GLM, we obtain the regression coefficients from

each PC. To convert the PCs' regression coefficient to the original variable regression coefficient, we use:

$$\hat{\beta}_i = \sum_{j=1}^r \hat{\alpha}_{ij} \hat{\gamma}_j \quad .i = 1, 2, \dots, p \tag{3}$$

where  $\hat{\gamma}_j$  is the regression coefficients of the  $j$ -th PC calculated in the GLM using hospitalization as response variable (Appendix 05),  $p$  is the number of covariates (total of 8),  $r$  is the number of PCs considered in the analysis, and  $\hat{\alpha}_{ij}$  is the  $j$ -th estimated eigenvector of the covariate's matrix (Appendix 06).  $\hat{\beta}_i$  is the individual contribution of each covariate (meteorology or air pollutant density) to the hospitalization (Appendix 07).

We use the first three PCs (Appendix 08) in the Poisson GLM because they explain most of the variance of the original covariates (up to 87%). We use the following software and Python (version 3.7) packages in the analysis: "scikit-learn v. 0.24", "pandas v. 1.3.1", and "statsmodels v. 0.12.2".

The risk analysis has been performed in this article according to:

$$\widehat{RR}_{(x_i)} \approx e^{x_i \hat{\beta}_i} \tag{4}$$

where,  $\widehat{RR}_{(x_i)}$  represent the Relative Risk (RR) for interquartile variation (3rd quantile - 1st quantile) of  $x_i$  (Appendix 09).

To deal with the problem of underestimating standard errors in the Poisson regression model when overdispersion is present, we used the Huber robust sandwich estimator, which corrects the heteroscedasticity from data. The method HC1 of Huber estimator from the Python statsmodel library has been used in this work (Palmer et al., 2013).

### 3. Results and discussion

Hospitalizations due to CVD and RSD are higher in less developed municipalities (i.e., for the lowest range of HDI – Figs. 3 and 4). The negative correlations between morbidity by RSD and CVD and HDI ( $\rho = -0.46$  and  $r = -0.41$ , respectively - Appendix 10) confirm that population living in more developed municipalities is less prone to cardiorespiratory hospitalization. In contrast, the positive correlation between HDI and  $O_3$ ,  $NO_2$ , and CO (Appendix 10) show that more developed municipalities are slightly more polluted than less developed ones (Appendix 11). Wealthier municipalities tend to have higher average levels of air pollutants density caused by the vehicular and industrial emissions (Hsiang et al., 2019).

To tease out the individual effects of air pollution and meteorology on health outcomes, we use the RR analysis derived from PCA-GLM. The RR analysis in Fig. 5 reveals that RSD is more susceptible to meteorology and air pollution than CVD since the risk values for RSD are larger than those for CVD. The inclusion of HDI as a covariate confirms that socioeconomic conditions have a strong effect on RSD and CVD, comparable to the effect of meteorological and air pollution variables (Fig. 5). Similarly, Laurent et al. (2007) demonstrated that groups with different socioeconomic conditions have different responses to air pollutant-related health effects; and Cakmak et al. (2016) showed that the risk of developing respiratory conditions increases in low-income and low-education groups our results corroborate finding from previous research that socioeconomic characteristics and climate could amplify or attenuate the air pollution effect on cardiovascular and respiratory mortality and morbidity (Cakmak et al., 2006, 2007).

Among air pollutants, the  $O_3$  and aerosol have the highest RR values, therefore, the highest impacts in respiratory and cardiovascular

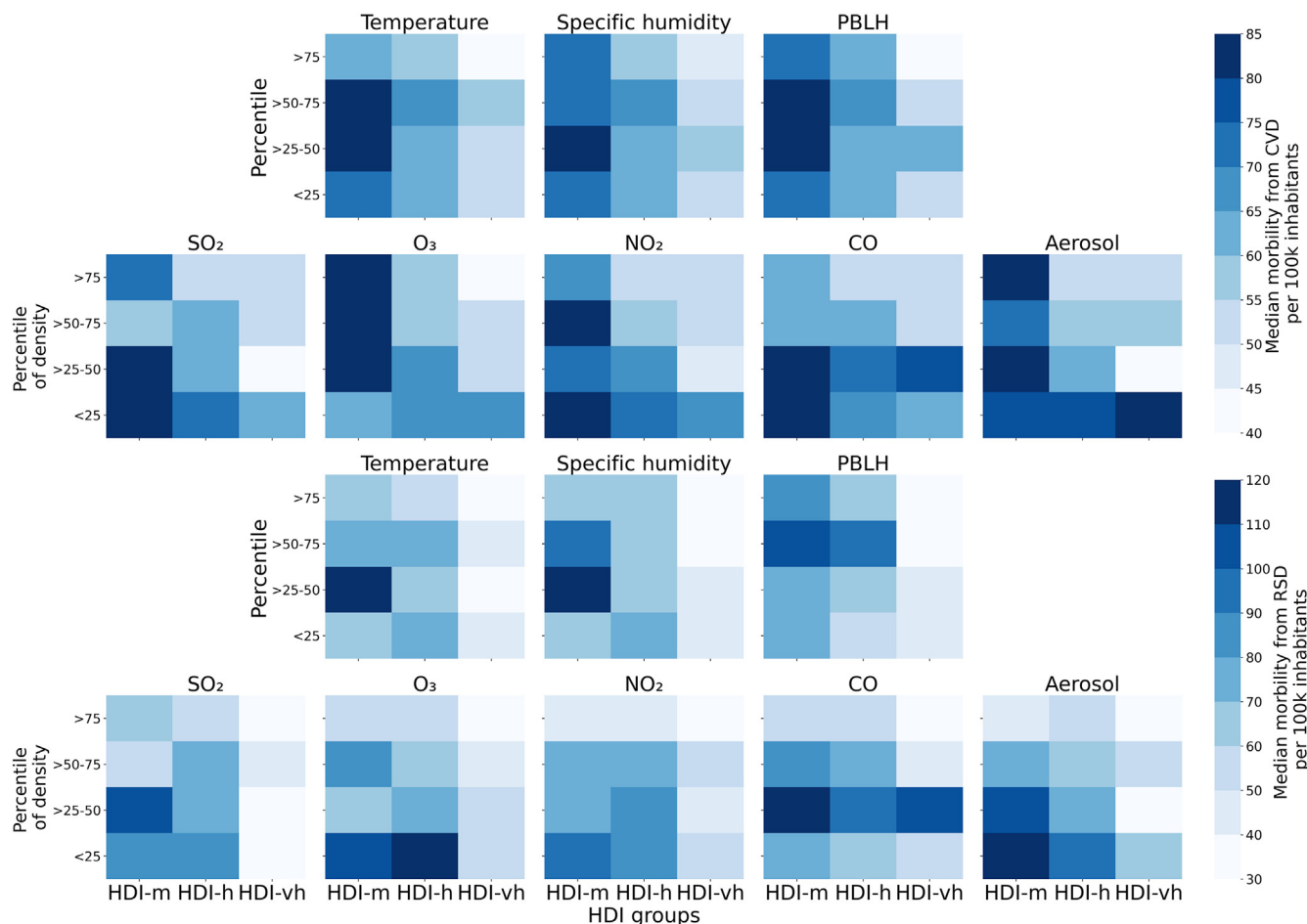
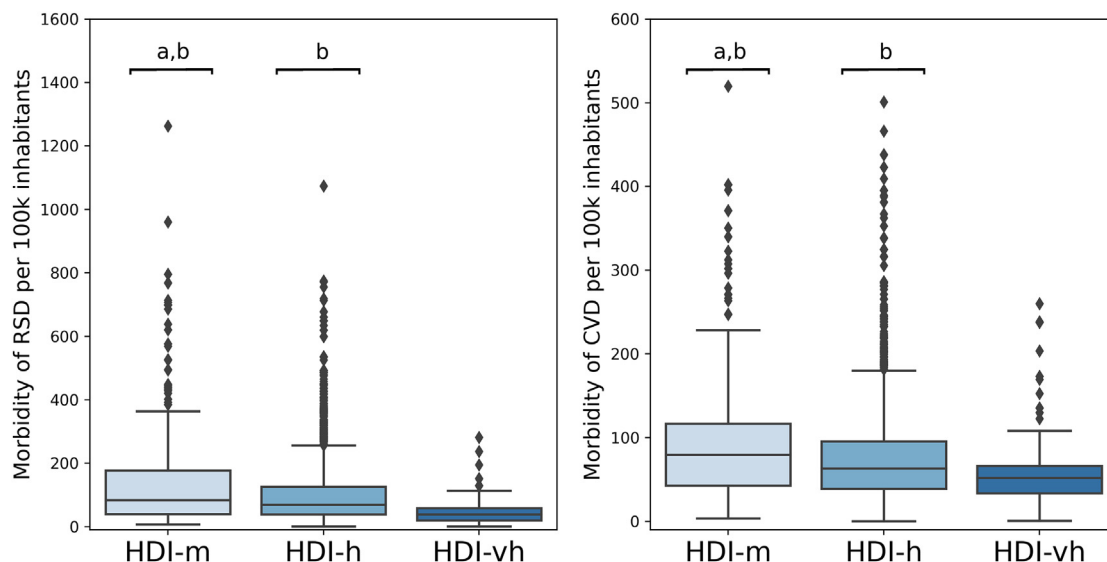


Fig. 3. Mosaic of median values of CVD (higher panels) and RSD (lower panels) morbidities for each HDI group (HDI-m (0.6 < HDI < 0.7), HDI-h (0.7 < HDI < 0.8), HDI-vh (HDI > 0.8)), according to percentiles classes of weather variables (temperature, specific humidity, PBL) and density of air pollutants (CO, O<sub>3</sub>, NO<sub>2</sub>, SO<sub>2</sub>, Aerosol).



**Fig. 4.** Boxplot of morbidity by RSD and CVD in SC classified according to HDI groups. HDI-m ( $0.6 < \text{HDI} < 0.7$ ), HDI-h ( $0.7 < \text{HDI} < 0.8$ ), HDI-vh ( $\text{HDI} > 0.8$ ); “a” is significantly different than HDI-h and “b” significantly different than HDI-vh (significance level  $p < 0.05$ ).

hospitalization (Fig. 5).  $\text{O}_3$  has also a marked effect on human health and is a major factor in asthma morbidity and mortality (WHO, 2021). It has been shown that the fine particles (aerodynamic diameter smaller than  $2.5 \mu\text{m}$ ) associated with the aerosol affects more people than any other pollutant (WHO, 2021). This parcel of the aerosol could be retained for a long time in the lung, inducing lung inflammation, cough, worsening asthma (Schraufnagel, 2020), and other health implications. Particulate matter has increased mortality due to lung cancer, ischemic heart disease, and chronic obstructive pulmonary disease (Cakmak et al., 2018).

Low temperature, humidity, and PBLH also affect CVD and RSD (Fig. 5). Temperature is the meteorological covariate with the stronger effect on cardiorespiratory hospitalization, followed by humidity. RSD hospitalizations are usually higher where the air is drier, which could amplify the effect of air pollution-related diseases (Leitte et al., 2009; Mäkinen et al., 2009).

The RR analysis by HDI range further corroborates that RSD hospitalization (Fig. 6) in municipalities with low socioeconomic conditions are more susceptible to the air pollutants density. We observe the largest RSD risk due to pollutants density in medium HDI municipalities. For all pollutant variables other than  $\text{NO}_2$  and  $\text{SO}_2$ , the relative risks show a clear pattern,

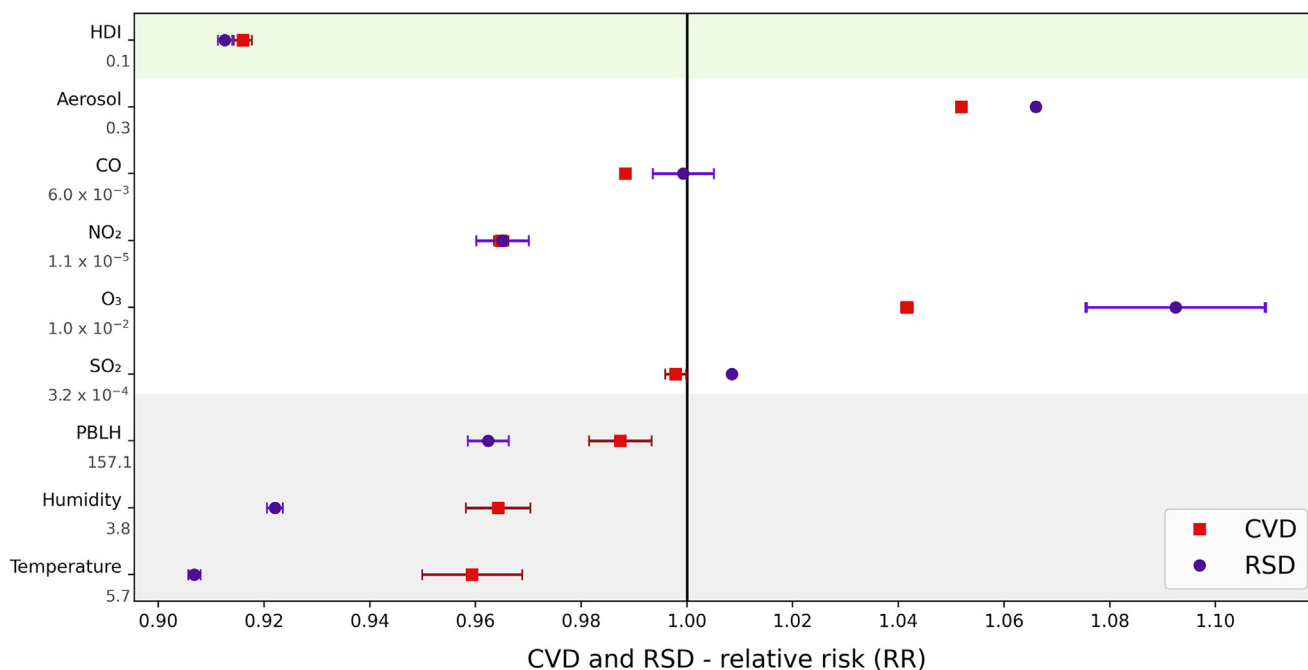


**Fig. 5.** Relative Risk (RR) for Respiratory System Disease (RSD) and Cardiovascular System Disease (CVD) due to HDI, temperature, humidity (Q), PBLH, and air pollutants density of  $\text{SO}_2$ ,  $\text{O}_3$ ,  $\text{NO}_2$ , CO, and Aerosol derived from PCA-GLM regression coefficients. The vertical line is the cutline between relative risks  $>1$  (positive associations) and relative risks  $<1$  (negative associations) associated with the respective covariate. Tails represent the confidence intervals from RR analysis which could also be found in appendix 13. Values below variable's name represent the original interquartile range of each variable used on RR estimates. Units from the interquartile ranges are the same as shown in Table 1.

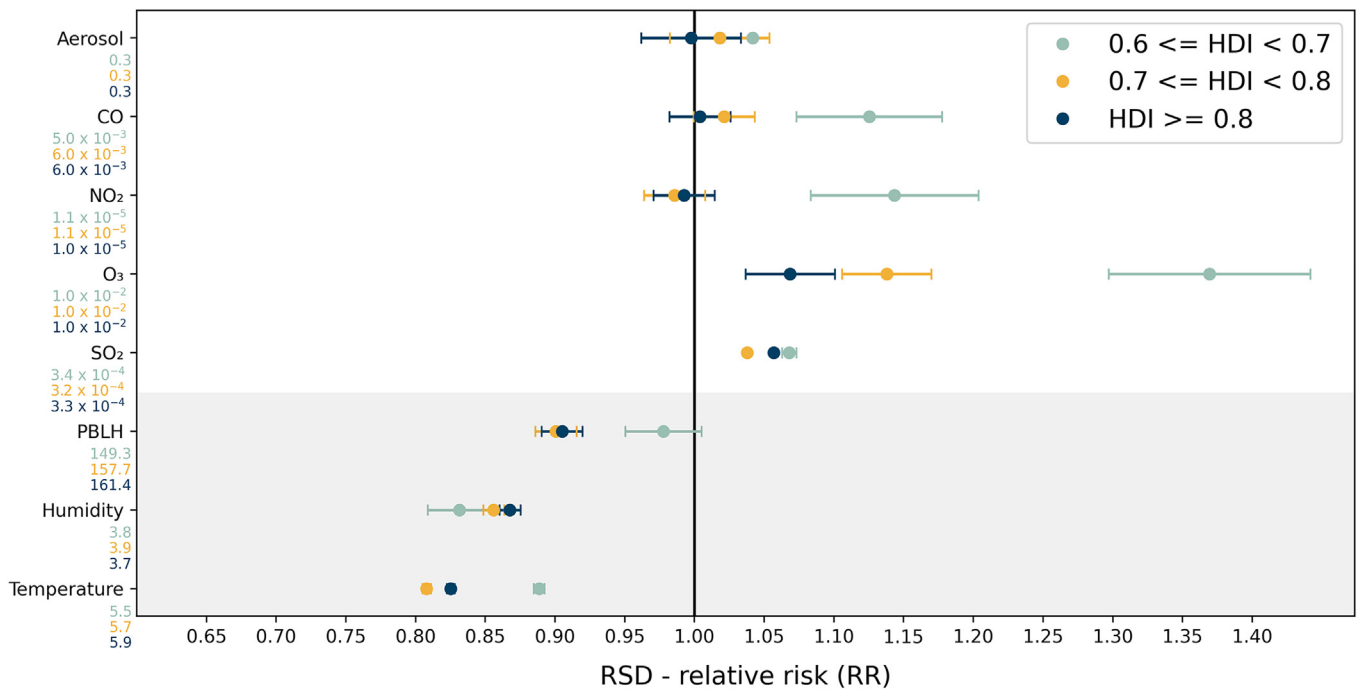


Fig. 6. Relative Risk (RR) for RSD due to temperature, humidity (Q), PBLH, and air pollutants density of SO<sub>2</sub>, O<sub>3</sub>, NO<sub>2</sub>, CO, and Aerosol for ranges of HDI derived from PCA-GLM regression coefficients. The vertical line is the cutline for the risk for negative (below 1.00) and positive (above 1.00) association related to the covariate. Tails represent the confidence intervals from RR analysis which could also be found in appendix 13. Values below variable's name represent the original interquartile range of each variable used on RR estimates. Units from the interquartile ranges are the same as shown in Table 1.

with relative risks being lowest in the highest HDI category, highest in the lowest HDI-category and intermediate in the medium HDI-category. As well as for fine particles and O<sub>3</sub>, it is widely reported that NO<sub>2</sub> (Meng et al., 2021), CO (Chen et al., 2021), and SO<sub>2</sub> (Amsalu et al., 2019; Orellano et al., 2021) has also increased the risk of RSD. It is worth emphasizing that even though the air pollutant density (Appendix 9) is smaller in municipalities in the medium HDI range, the RR values are slightly higher than in the high HDI range. It confirms that the impact on RSD is higher in vulnerable municipalities, even when air pollution is lower.

Low temperature, humidity, and PBLH increase the risk of RSD, especially in medium and high HDI ranges, which is in agreement with previous research (e.g., Giang et al., 2014; Mäkinen et al., 2009; Tsangari et al., 2016; Zhao et al., 2019). The analysis also reveals that temperature, humidity, and PBLH impose similar pressure on RSD hospitalization risk as the air pollutant densities. The only exception is the RR due to O<sub>3</sub> in the medium HDI range which is much higher than the other covariates.

The ratio of hospitalization by pollutant density and meteorology variation, expressed by  $\hat{\beta}_i$  values also confirms that the medium range HDI group is more susceptible to RSD due to the air pollutants density (Appendix 12). In this context, Cakmak et al. (2006) have shown that living in communities in which individuals have lower household education and income levels may increase the individuals' vulnerability to air pollution.

When analyzing the RR of CVD by a group of HDI (Fig. 7), O<sub>3</sub> has the highest overall RR value among pollutants, followed by SO<sub>2</sub>, CO, Aerosol, and NO<sub>2</sub>. In this case, the effect on CVD admissions is highest in the highest HDI-category for SO<sub>2</sub>, O<sub>3</sub> and CO, where the air pollution is also higher, and the population is older. This should be further investigated using a larger dataset, covering a larger period and municipalities. Temperature is the meteorological covariate with the lowest overall RR (highest relative risk for low temperatures) for CVD by HDI group. The risk of CVD increases with the decrease in the temperature in all groups and is higher in very-high HDI ranges.

We do not include confounding factors other than HDI in our analysis, such as age, height, weight, body mass index, occupation, gestational, hypertension, gender, number of neonates, and others. It is a limitation of our study and could be addressed in future studies and when these data become available. Future work would better elucidate the air pollution and

meteorology effect among HDI ranges using a larger dataset covering entire country and time window.

Although we have used PBLH as a proxy of air quality, it does not capture seasonal variations in emissions. Therefore, the association between PBLH and air quality should be carefully analyzed with future work including the effect of seasonal variations in emissions and the effect of boundary layer variations in air quality.

#### 4. Conclusion

In this work, we evaluate the effect of air pollution and meteorological conditions on cardiorespiratory diseases combining satellite images from Sentinel-5 and meteorological data from the WRF model. Our results reveal that socioeconomic development plays an important role in determining the air pollution and meteorological drivers of hospitalization in southern Brazil. Developed municipalities are more polluted, however, they have less cardiorespiratory hospitalizations.

Our results suggest that RSD hospitalization in Southern Brazil is impacted by air pollutant density, low temperature, low humidity, and low PBLH, especially in low socioeconomic municipalities. O<sub>3</sub> and aerosol are the most important among the pollutants, while the temperature is the most relevant meteorological variable on RSD and CVD risks. Comparing both diseases, RSD is more susceptible to meteorology and air pollution than CDV. Regarding CVD hospitalization, air pollution density affects with the similar strength as meteorology, confirming that air pollution is one of the most important environmental cardiovascular risk factors. The analysis dividing the data by group of HDI reveals that CVD risk is higher in very high HDI municipalities, where the air pollution is higher, and the population is older. It should be further investigated using a larger dataset, covering a larger period and municipalities.

Our results indicate that socioeconomic development is a key predictor of RSD and CVD morbidities. Future work using a larger dataset should include long-term exposition, chronicle effects, and other influencing factors (e.g., genetics, life stage, sex, and comorbidities). We also recommend further studies including the effect of seasonal variations in emissions and the effect of boundary layer variations in air quality.

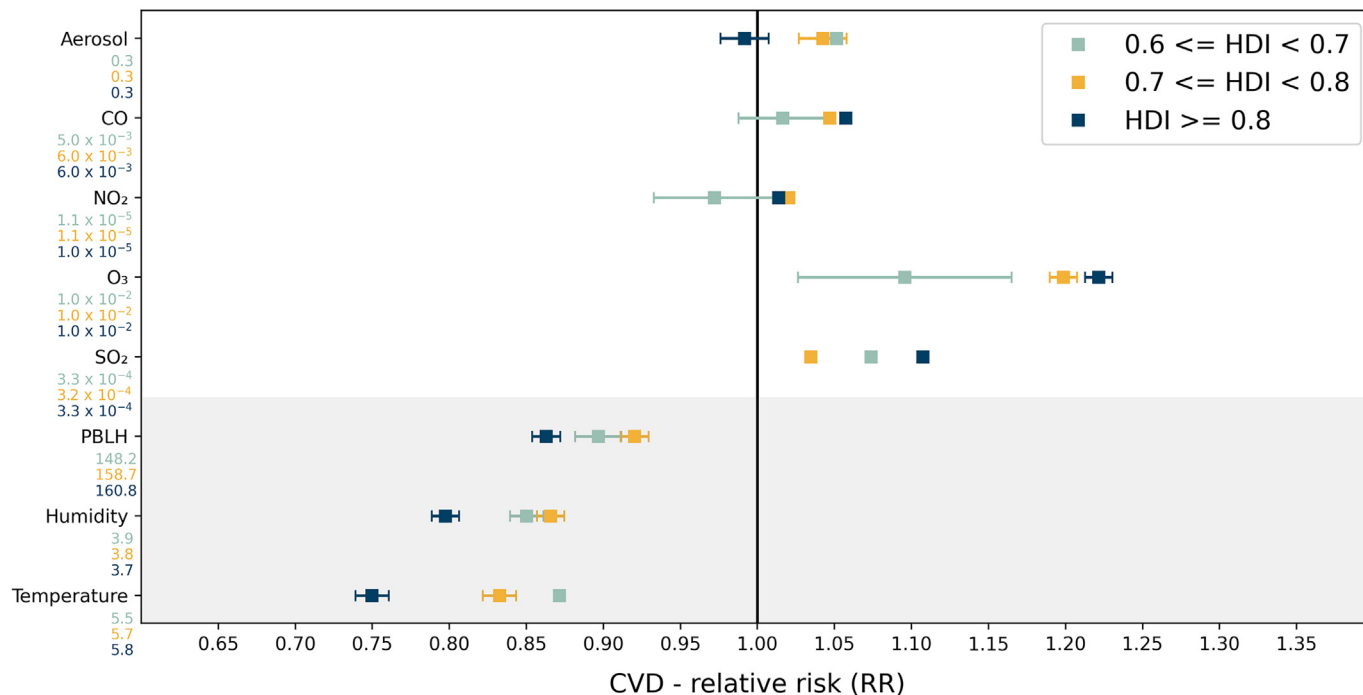


Fig. 7. Relative Risk (RR) for CVD due to temperature, humidity (Q), PBLH, and air pollutants density of SO<sub>2</sub>, O<sub>3</sub>, NO<sub>2</sub>, CO, and Aerosol for ranges of HDI derived from PCA-GLM regression coefficients. The vertical line is the cutline for the risk for negative (below 1.00) and positive (above 1.00) association related to the covariate. Tails represent the confidence intervals from RR analysis which could also be found in appendix 13. Values below variable's name represent the original interquartile range of each variable used on RR estimates. Units from the interquartile ranges are the same as shown in Table 1.

#### CRedit authorship contribution statement

**Robson Will:** Conceptualization, Methodology, Formal analysis, Investigation, Writing – original draft, Writing – review & editing, Visualization. **Marina Hirota:** Writing – review & editing, Visualization. **Pedro Luiz Borges Chaffe:** Conceptualization, Investigation, Writing – original draft, Writing – review & editing, Visualization. **Otavio Nunes dos Santos:** Methodology, Formal analysis, Writing – review & editing, Visualization. **Leonardo Hoinaski:** Conceptualization, Methodology, Formal analysis, Investigation, Writing – original draft, Writing – review & editing, Visualization.

#### Declaration of competing interest

The authors declare that they have no known competing financial interests or personal relationships that could have appeared to influence the work reported in this paper.

#### Acknowledgments

Authors would like to thank the Fundação de Amparo à Pesquisa e Inovação de Santa Catarina - FAPESC, for financial support of project number 2018TR499 (“Avaliação do impacto das emissões veiculares, queimadas, industriais e naturais na qualidade do ar em Santa Catarina”).

#### Appendix A. Appendices. Supplementary data

Supplementary data to this article can be found online at <https://doi.org/10.1016/j.scitotenv.2022.154063>.

#### References

Alvares, C.A., Stape, J.L., Sentelhas, P.C., De Moraes Gonçalves, J.L., Sparovek, G., 2013. Köppen's climate classification map for Brazil. *Meteorol. Zeitschrift* 22, 711–728. <https://doi.org/10.1127/0941-2948/2013/0507>.

- Amsalu, E., Guo, Y., Li, H., Wang, T., Liu, Y., Wang, A., Liu, X., Tao, L., Luo, Y., Zhang, F., Yang, X., Li, X., Wang, W., Guo, X., 2019. Short-term effect of ambient sulfur dioxide (SO<sub>2</sub>) on cause-specific cardiovascular hospital admission in Beijing, China: a time series study. *Atmos. Environ.* 208, 74–81. <https://doi.org/10.1016/j.atmosenv.2019.03.015>.
- Andréão, W.L., Toledo de Almeida Albuquerque, T., 2021. Avoidable mortality by implementing more restrictive fine particles standards in Brazil: an estimation using satellite surface data. *Environ. Res.* 192. <https://doi.org/10.1016/j.envres.2020.110288>.
- Borsdorff, T., Aan de Brugh, J., Hu, H., Aben, I., Hasekamp, O., Landgraf, J., 2018. Measuring carbon monoxide with TROPOMI: first results and a comparison with ECMWF-IFS analysis data. *Geophys. Res. Lett.* 45, 2826–2832. <https://doi.org/10.1002/2018GL077045>.
- Brasil, 2020. TabNet Win32 3.0: Morbidade Hospitalar do SUS - por local de residência - Santa Catarina [WWW Document]. URL <http://tabnet.datasus.gov.br/cgi/deftohtm.exe?sih/cnv/nrsc.def> (accessed 10.12.20).
- Cakmak, S., Dales, R.E., Judek, S., 2006. Respiratory health effects of air pollution gases: modification by education and income. *Arch. Environ. Occup. Health* 61, 5–10. <https://doi.org/10.3200/AEOH.61.1.5-10>.
- Cakmak, S., Dales, R.E., Vidal, C.B., 2007. Air pollution and mortality in Chile: susceptibility among the elderly. *Environ. Health Perspect.* 115, 524–527. <https://doi.org/10.1289/ehp.9567>.
- Cakmak, S., Hebborn, C., Cakmak, J.D., Vanos, J., 2016. The modifying effect of socioeconomic status on the relationship between traffic, air pollution and respiratory health in elementary schoolchildren. *J. Environ. Manag.* 177, 1–8. <https://doi.org/10.1016/j.jenvman.2016.03.051>.
- Cakmak, S., Hebborn, C., Pinault, L., Lavigne, E., Vanos, J., Crouse, D.L., Tjepkema, M., 2018. Associations between long-term PM<sub>2.5</sub> and ozone exposure and mortality in the Canadian Census Health and Environment Cohort (CANHEC), by spatial synoptic classification zone. *Environ. Int.* 111, 200–211. <https://doi.org/10.1016/j.envint.2017.11.030>.
- Chen, K., Breitner, S., Wolf, K., Stafoggia, M., Sera, F., Vicedo-Cabrera, A.M., Guo, Y., Tong, S., Lavigne, E., Matus, P., Valdés, N., Kan, H., Jaakkola, J.J.K., Rytty, N.R.I., Huber, V., Scortichini, M., Hashizume, M., Honda, Y., Nunes, B., Madureira, J., Holobăcă, L.H., Fratianni, S., Kim, H., Lee, W., Tobias, A., Íñiguez, C., Forsberg, B., Åström, C., Ragetti, M.S., Guo, Y.L.L., Chen, B.Y., Li, S., Milojevic, A., Zanobetti, A., Schwartz, J., Bell, M.L., Gasparrini, A., Schneider, A., 2021. Ambient carbon monoxide and daily mortality: a global time-series study in 337 cities. *Lancet Planet. Heal.* 5, e191–e199. [https://doi.org/10.1016/S2542-5196\(21\)00026-7](https://doi.org/10.1016/S2542-5196(21)00026-7).
- Clougherty, J.E., 2010. A growing role for gender analysis in air pollution epidemiology. *Environ. Health Perspect.* 118, 167–176. <https://doi.org/10.1289/ehp.0900994>.
- ce:label>Ebisu et al., 2019Ebisu, K., Malig, B., Hasheminassab, S., Sioutas, C., 2019. Age-specific seasonal associations between acute exposure to PM<sub>2.5</sub> sources and cardiorespiratory hospital admissions in California. *Atmos. Environ.* 218, 117029. <https://doi.org/10.1016/j.atmosenv.2019.117029>.
- European Environment Agency, 2018. Unequal Exposure and Unequal Impacts: Social Vulnerability to Air Pollution, Noise and Extreme Temperatures in Europe. , pp. 1–102 <https://doi.org/10.2800/324183>.

- Gao, Y., Chan, E.Y.Y., Zhu, Y., Wong, T.W., 2013. Adverse effect of outdoor air pollution on cardiorespiratory fitness in Chinese children. *Atmos. Environ.* 64, 10–17. <https://doi.org/10.1016/j.atmosenv.2012.09.063>.
- Gasparrini, A., Guo, Y., Hashizume, M., Lavigne, E., Zanobetti, A., Schwartz, J., Tobias, A., Tong, S., Rocklöv, J., Paulo, S., Paulo, S., 2015. Mortality risk attributable to high and low ambient temperature: a multicountry observational study. *Lancet* 369–375. [https://doi.org/10.1016/S0140-6736\(14\)62114-0](https://doi.org/10.1016/S0140-6736(14)62114-0).
- Giang, P.N., Van Dung, D., Giang, K.B., Van Vinh, H., Rocklöv, J., 2014. The effect of temperature on cardiovascular disease hospital admissions among elderly people in Thai Nguyen Province, Vietnam. *Glob. Health Action* 7, 1–7. <https://doi.org/10.3402/gha.v7.23649>.
- Goldberg, D.L., Lu, Z., Streets, D.G., De Foy, B., Griffin, D., McLinden, C.A., Lamsal, L.N., Krotkov, N.A., Eskes, H., 2019. Enhanced capabilities of TROPOMI NO<sub>2</sub>: estimating NOX from North American cities and power plants. *Environ. Sci. Technol.* 53, 12594–12601. <https://doi.org/10.1021/acs.est.9b04488>.
- Ho, H.C., Wong, M.S., Yang, L., Chan, T.C., Bilal, M., 2018. Influences of socioeconomic vulnerability and intra-urban air pollution exposure on short-term mortality during extreme dust events. *Environ. Pollut.* 235, 155–162. <https://doi.org/10.1016/j.envpol.2017.12.047>.
- Hsiang, S., Oliva, P., Walker, R., 2019. The distribution of environmental damages. *Rev. Environ. Econ. Policy* 13, 83–103. <https://doi.org/10.1093/reep/rey024>.
- IBGE, 2013. *Índice de Desenvolvimento Humano Municipal Brasileiro, Atlas do Desenvolvimento Humano no Brasil*.
- IBGE, 2020. *IBGE | Cidades@ | Santa Catarina | Panorama [WWW Document]*. URL <https://cidades.ibge.gov.br/brasil/sc/panorama> (accessed 9.13.21).
- Ikäheimo, T.M., Jokelainen, J., Näyhä, S., Laatikainen, T., Jousilahti, P., Laukkanen, J., Jaakkola, J.J.K., 2020. Cold weather-related cardiorespiratory symptoms predict higher morbidity and mortality. *Environ. Res.* 191. <https://doi.org/10.1016/j.envres.2020.110108>.
- Krall, J.R., Chang, H.H., Waller, L.A., Mulholland, J.A., Winquist, A., Talbot, E.O., Rager, J.R., Tolbert, P.E., Sarnat, S.E., 2018. A multicity study of air pollution and cardiorespiratory emergency department visits: comparing approaches for combining estimates across cities. *Environ. Int.* 120, 312–320. <https://doi.org/10.1016/j.envint.2018.07.033>.
- Laurent, O., Bard, D., Filleul, L., Segala, C., 2007. Effect of socioeconomic status on the relationship between atmospheric pollution and mortality. *J. Epidemiol. Community Health* 61, 665–675. <https://doi.org/10.1136/jech.2006.053611>.
- Leitte, A.M., Petrescu, C., Franck, U., Richter, M., Suci, O., Ionovici, R., Herbarth, O., Schlink, U., 2009. Respiratory health, effects of ambient air pollution and its modification by air humidity in Drobeta-Turnu Severin, Romania. *Sci. Total Environ.* 407, 4004–4011. <https://doi.org/10.1016/j.scitotenv.2009.02.042>.
- Mäkinen, T.M., Juvonen, R., Jokelainen, J., Harju, T.H., Peitso, A., Bloigu, A., Silvennoinen-Kassinen, S., Leinonen, M., Hassi, J., 2009. Cold temperature and low humidity are associated with increased occurrence of respiratory tract infections. *Respir. Med.* 103, 456–462. <https://doi.org/10.1016/j.rmed.2008.09.011>.
- Meng, X., Liu, C., Chen, R., Sera, F., Vicedo-Cabrera, A.M., Milojevic, A., Guo, Y., Tong, S., De Sousa Zanotti Stagliorio Coelho, M., Saldiva, P.H.N., Lavigne, E., Correa, P.M., Ortega, N.V., Osorio, S., Garcia, Kysely, J., Urban, A., Orru, H., Maasikmets, M., Jaakkola, J.J.K., Ryti, N., Huber, V., Schneider, A., Katsouyanni, K., Analitis, A., Hashizume, M., Honda, Y., Ng, C.F.S., Nunes, B., Teixeira, J.P., Holobaca, I.H., Fratianne, S., Kim, H., Tobias, A., Iñiguez, C., Forsberg, B., Åström, C., Ragetli, M.S., Guo, Y.L.L., Pan, S.C., Li, S., Bell, M.L., Zanobetti, A., Schwartz, J., Wu, T., Gasparrini, A., Kan, H., 2021. Short term associations of ambient nitrogen dioxide with daily total, cardiovascular, and respiratory mortality: multilocation analysis in 398 cities. *BMJ* <https://doi.org/10.1136/bmj.n534>.
- Orellano, P., Reynoso, J., Quaranta, N., 2021. Short-term exposure to sulphur dioxide (SO<sub>2</sub>) and all-cause and respiratory mortality: a systematic review and meta-analysis. *Environ. Int.* 150, 106434. <https://doi.org/10.1016/j.envint.2021.106434>.
- Palmer, A., Losilla, J.M., Vives, J., Jimenez, R., 2013. Erratum: Overdispersion in the poisson regression model. A comparative simulation study (*Methodology* (2007) 3:3 (89–99) DOI:10.1027/1614-2241.3.3.89). *Methodology* 9, 178. <https://doi.org/10.1027/1614-2241/a000069>.
- Pino-Cortés, E., Díaz-Robles, L.A., Campos, V., Vallejo, F., Cubillos, F., Gómez, J., Cereceda-Balic, F., Fu, J., Carrasco, S., Figueroa, J., 2020. Effect of socioeconomic status on the relationship between short-term exposure to PM<sub>2.5</sub> and cardiorespiratory mortality and morbidity in a megacity: the case of Santiago de Chile. *Air Qual. Atmos. Heal.* 13, 509–517. <https://doi.org/10.1007/s11869-020-00818-6>.
- PNUD, Ipea, F., 2013. *Índice de Desenvolvimento Humano Municipal Brasileiro, Atlas do Desenvolvimento Humano no Brasil*.
- Requia, W.J., Koutrakis, P., Roig, H.L., Adams, M.D., Santos, C.M., 2016. Association between vehicular emissions and cardiorespiratory disease risk in Brazil and its variation by spatial clustering of socio-economic factors. *Environ. Res.* 150, 452–460. <https://doi.org/10.1016/j.envres.2016.06.027>.
- Righini, G., Cappelletti, A., Ciucci, A., Cremona, G., Piersanti, A., Vitali, L., Ciancarella, L., 2014. GIS based assessment of the spatial representativeness of air quality monitoring stations using pollutant emissions data. *Atmos. Environ.* 97, 121–129. <https://doi.org/10.1016/j.atmosenv.2014.08.015>.
- de Rocha, I.O., 2019. *Atlas Geográfico de Santa Catarina: população – fascículo 3, Secretaria de Estado do Planejamento, Diretoria de Estatística e Cartografia*. <https://doi.org/10.5965/978858302152032018>.
- Schraufnagel, D.E., 2020. The health effects of ultrafine particles. *Exp. Mol. Med.* 52, 311–317. <https://doi.org/10.1038/s12276-020-0403-3>.
- Skamarock, W.C., Klemp, J.B., Dudhia, J., Gill, D.O., Barker, D., Duda, M.G., Huang, X., Wang, W., Powers, J.G., 2008. A description of the advanced research WRF version 3 (No. NCAR/TN-475+STR). *Univ. Corp. Atmos. Res.* <https://doi.org/10.1080/07377366.2001.10400427>.
- Skamarock, W.C., Klemp, J.B., Dudhia, J., Gill, D.O., Zhiquan, L., Berner, J., Wang, W., Powers, J.G., Duda, M.G., Barker, D.M., Huang, X.-Y., 2019. A Description of the Advanced Research WRF Model Version 4. *NCAR Tech. Note NCAR/TN-475+STR*, p. 145 <https://doi.org/10.5065/1dfh-6p97>.
- Strak, M., Janssen, N., Beelen, R., Schmitz, O., Karssenberg, D., Houthuijs, D., van den Brink, C., Dijst, M., Brunekreef, B., Hoek, G., 2017. Associations between lifestyle and air pollution exposure: potential for confounding in large administrative data cohorts. *Environ. Res.* 156, 364–373. <https://doi.org/10.1016/j.envres.2017.03.050>.
- Sun, Z., Yang, L., Bai, X., Du, W., Shen, G., Fei, J., Wang, Y., Chen, A., Chen, Y., Zhao, M., 2019. Maternal ambient air pollution exposure with spatial-temporal variations and pre-term birth risk assessment during 2013–2017 in Zhejiang Province, China. *Environ. Int.* 133, 105242. <https://doi.org/10.1016/j.envint.2019.105242>.
- Tobias, A., Saez, M., 2004. *Time-Series Regression Models to Study the Short-Term Effects of Environmental Factors on Health \* 1–21*.
- Toro, R., A, Kvakic, M., Klaić, Z.B., Koraćin, D., Morales, R.G.E., S, Leiva, M.A., G, 2019. Exploring atmospheric stagnation during a severe particulate matter air pollution episode over complex terrain in Santiago, Chile. *Environ. Pollut.* 244, 705–714. <https://doi.org/10.1016/j.envpol.2018.10.067>.
- Tsangari, H., Paschalidou, A.K., Kassomenos, A.P., Vardoulakis, S., Heaviside, C., Georgiou, K.E., Yamasaki, E.N., 2016. Extreme weather and air pollution effects on cardiovascular and respiratory hospital admissions in Cyprus. *Sci. Total Environ.* 542, 247–253. <https://doi.org/10.1016/j.scitotenv.2015.10.106>.
- WHO, 2017. *O Impacto Global da Doença Respiratória, European Respiratory Society*.
- WHO, 2021. *Ambient (Outdoor) Air Pollution [WWW Document]*. URL [https://www.who.int/news-room/fact-sheets/detail/ambient-\(outdoor\)-air-quality-and-health](https://www.who.int/news-room/fact-sheets/detail/ambient-(outdoor)-air-quality-and-health) (accessed 12.6.21).
- Yatkin, S., Gerboles, M., Belis, C.A., Karagulian, F., Lagler, F., Barbieri, M., Borowiak, A., 2020. Representativeness of an air quality monitoring station for PM<sub>2.5</sub> and source apportionment over a small urban domain. *Atmos. Pollut. Res.* 11, 225–233. <https://doi.org/10.1016/j.apr.2019.10.004>.
- Zhao, Y., Zhang, L., Zhou, M., Chen, D., Lu, X., Tao, W., Liu, J., Tian, H., Ma, Y., Fu, T.M., 2019. Influences of planetary boundary layer mixing parameterization on summertime surface ozone concentration and dry deposition over North China. *Atmos. Environ.* 218, 116950. <https://doi.org/10.1016/j.atmosenv.2019.116950>.
- Zhao, F., Liu, C., Cai, Z., Liu, X., Bak, J., Kim, J., Hu, Q., Xia, C., Zhang, C., Sun, Y., Wang, W., Liu, J., 2021. Ozone profile retrievals from TROPOMI: implication for the variation of tropospheric ozone during the outbreak of COVID-19 in China. *Sci. Total Environ.* 764, 142886. <https://doi.org/10.1016/j.scitotenv.2020.142886>.